

Entanglement Dynamics in Dispersive Optomechanics: Non-Classicality and Revival

Igor Brandão,^{*} Bruno Suassuna,[†] Bruno Melo,[‡] and Thiago Guerreiro[§]

Department of Physics, Pontifical Catholic University of Rio de Janeiro, Rio de Janeiro 22451-900, Brazil

We study entanglement dynamics in a dispersive optomechanical system consisting of two optical modes and a mechanical oscillator inside an optical cavity. The two optical modes interact with the mechanical oscillator, but not directly with each other. The appearance of optical entanglement witnesses non-classicality of the oscillator. We study the dependence of the entanglement dynamics with the optomechanical coupling, the mean cavity photon numbers and temperature. We propose an experimental realization with ultracold atomic ensembles.

Introduction — Entanglement is one of the most striking phenomena of quantum theory [1]. Generating, manipulating and measuring entanglement in systems with many constituents and with a large number of degrees of freedom is one of the challenges of Quantum Information and Metrology [2], and an interesting frontier in Fundamental Physics [3]. In particular, entangling massive objects could open the way to interesting tests of quantum theory [4, 5] and experiments aimed at probing gravitational effects of quantum mechanical matter [6–12].

It is well known that entanglement of massive objects can be realized in quantum cavity optomechanical experiments [13]. For instance, a cavity with a moving end mirror can be used to generate entangled “cat states” of both light [14, 15] and matter [16–19]. Similar systems have also been proposed as an effective nonlinear medium [20–22] and squeezing [23–25] as well as optical entanglement [26] have been experimentally demonstrated in a variety of set-ups such as cavity cold atomic ensembles [27], dispersive dielectric membranes [28] and silicon micro-resonators [29].

Certifying quantumness of optomechanical systems, however, is a far-from-obvious task. Relations among entanglement and non-classicality measures of quantum states can be used to probe the quantum nature of inaccessible objects such as a harmonic oscillator in an optical cavity [30]. Recurrence of optical squeezing in a cavity with a moving mirror has also been proposed as a witness of non-classicality [31] and it has been shown that when two subsystems locally interact with a third one, but not directly with each other, the appearance of entanglement among those subsystems is sufficient to prove non-classicality of the third party [32]. Building on some of these ideas the present work studies the intricate entanglement dynamics of a dispersive optomechanical system, how to use that dynamics to probe the quantum nature of the oscillator when only optical degrees of freedom are accessible and how to optimize the generated optical entanglement by careful choice of the optomechanical coupling and the number of photons in an experiment.

Considering as possible implementations levitated op-

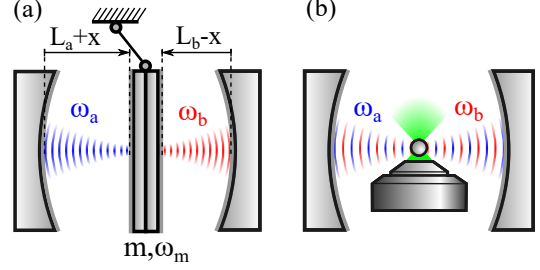


FIG. 1: (a) Schematics of coupled optical cavities sharing a “mirror-in-the-middle” under a harmonic potential. No photon transfer from one cavity to the other is allowed. (b) Schematics of a particle trapped by an optical tweezer coupled to two modes of a cavity. The particle can be considered as a Silica nano-sphere or a cloud of ultracold atoms. When the levitated object is properly positioned, the Hamiltonian describing both systems acquires the same form.

tomechanical systems such as Silica nano-spheres or cold atomic ensembles and a “two-sided” cavity with a moving mirror in the middle, we map how entanglement and entropy appear and evolve among the various optical and mechanical subsystems for different optomechanical coupling strengths and optical field intensities. The appearance of mechanically induced optical entanglement and its subsequent death and revival are generic in these systems, implying quantization of the center-of-mass motion of the moving object. We also point that under certain circumstances entanglement seems to “flow” through different subsystems, and such dynamics can be used to infer non-classicality and entanglement among different components of the system. We consider examples of both non-Gaussian and Gaussian initial quantum states, for which we study the dynamics of concurrence and logarithmic negativity, respectively. An experimental realization using levitated cold atomic ensembles is proposed.

Hamiltonian description — The system we are primarily interested in is shown in Figure 1(a): two optical cavities, of lengths L_a and L_b , are populated by modes of frequencies ω_a and ω_b and share a common perfect movable mirror of mass m subject to a harmonic potential of frequency ω_m . We refer to this as the “mirror-in-the-middle” configuration. In this system the optical modes

never interact directly, except via the dispersive coupling due to the presence of the mechanical mode. Since we are interested in studying entanglement dynamics in optomechanics, we shall assume the cavities can be initialized in particular states and the laser driving-term can be turned off during the course of the experiment. It is also assumed that optical losses are negligible during the time of the experiment and a discussion of the conditions under which this is true and the experimental feasibility is addressed in the experimental proposal.

The Hamiltonian of the system reads [13]

$$\frac{H}{\hbar} = \omega_a \hat{a}^\dagger \hat{a} + \omega_b \hat{b}^\dagger \hat{b} + \omega_m \hat{c}^\dagger \hat{c} - g_{0,a} \hat{a}^\dagger \hat{a} (\hat{c}^\dagger + \hat{c}) + g_{0,b} \hat{b}^\dagger \hat{b} (\hat{c}^\dagger + \hat{c}), \quad (1)$$

where $g_{0,i} = \omega_i x_{zpf} / L_i$ are the optomechanical couplings, with $x_{zpf} = \sqrt{\hbar / 2m\omega_m}$ the zero point fluctuation of the mirror and \hat{a} , \hat{b} , \hat{c} (\hat{a}^\dagger , \hat{b}^\dagger , \hat{c}^\dagger) are the annihilation (creation) operators of each optical and mechanical modes, denoted by A , B and C , respectively. Such Hamiltonian can also be implemented using a cavity with a levitated nano-particle [33–35] or an ultracold atom cloud [27, 36, 37] properly positioned along the cavity axis. This is illustrated in Figure 1(b); see the Supplemental Material for details on implementations.

Assuming equal frequencies for the optical modes $\omega_a = \omega_b$, and approximately equal cavity lengths $L_a \sim L_b$ we may simplify the notation and directly write $g_0 \equiv g_{0,a} \sim g_{0,b}$. The unitary evolution operator resulting from equation (1) becomes

$$\hat{U}(t) = e^{-ir_a \hat{a}^\dagger \hat{a} t} e^{-ir_b \hat{b}^\dagger \hat{b} t} e^{-iB(t)(\hat{a}^\dagger \hat{a} - \hat{b}^\dagger \hat{b})^2} e^{+k\hat{a}^\dagger \hat{a}(\eta \hat{c}^\dagger - \eta^* \hat{c})} e^{-k\hat{b}^\dagger \hat{b}(\eta \hat{c}^\dagger - \eta^* \hat{c})} e^{-i\hat{c}^\dagger \hat{c} t}, \quad (2)$$

where we define the dimensionless optomechanical coupling $k = g_0 / \omega_m$, $r_i = \omega_i / \omega_m$, the scaled time $\omega_m t \rightarrow t$, and the functions $\eta(t) = 1 - e^{-it}$ and $B(t) = -k^2(t - \sin t)$. Note the evolution operator is comprised of a *Kerr-like* term, responsible for an effective optical non-linearity [38], as well as an *optically-driven* displacement operator acting on the mechanical mode.

We expect that a generic separable state evolves into an entangled state by the unitary evolution above. This is not always the case, as can be seen by considering the energy eigenstates of the system

$$\hat{\mathcal{D}}_C(k(n_A - m_B)) |n_A, m_B, \ell_C\rangle, \quad (3)$$

where $\{|n_A, m_B, \ell_C\rangle\}$ denotes the number basis and $\hat{\mathcal{D}}_C(\alpha)$ the displacement operator acting on the mechanical oscillator, mode C , by a displacement $\alpha \in \mathbb{C}$. See the Supplemental Material for a derivation of equation (2) and of the energy eigenstates above.

Non-Gaussian states — Consider that the cavities in Figure 1(a) are initially populated by the non-Gaussian

state

$$|\Psi(0)\rangle = \left(\frac{|0\rangle + |1\rangle}{\sqrt{2}} \right) \otimes \left(\frac{|0\rangle + |1\rangle}{\sqrt{2}} \right) \otimes |0\rangle. \quad (4)$$

These states can be prepared in an approximate way using photon pair sources and displacement-based detection [39, 40] or non-linear light-matter interactions in cavity quantum electrodynamics [41, 42]. The “mirror-in-the-middle” is taken to be in the ground state for simplicity; in the next section we shall consider the effects of a finite temperature oscillator. Notice the initial state is separable and hence the appearance of entanglement between modes A and B would evidence the non-classical nature of mode C [32]. Time evolution of (4) in the interaction picture is explicitly given by

$$|\Psi(t)\rangle = \frac{|00\rangle}{2} |0\rangle + e^{iB(t)} \frac{|01\rangle}{2} \hat{\mathcal{D}}_C(k\xi(t)) |0\rangle + e^{iB(t)} \frac{|10\rangle}{2} \hat{\mathcal{D}}_C(-k\xi(t)) |0\rangle + \frac{|11\rangle}{2} |0\rangle, \quad (5)$$

where $\xi(t) = e^{it}\eta(t)$. It is expected that the evolved state (5) exhibits entanglement between modes A and B . This can be promptly seen by noticing that coherent states are non-orthogonal and, in the limit of small coupling k , the state assumes the form $|\Psi(t)\rangle \simeq |\varphi_{AB}\rangle \otimes |\varphi_C\rangle$, where

$$|\varphi_{AB}\rangle \simeq \frac{|0\rangle}{2} \left(|0\rangle + e^{iB(t)} |1\rangle \right) + e^{iB(t)} \frac{|1\rangle}{2} \left(|0\rangle + e^{-iB(t)} |1\rangle \right) \quad (6)$$

and $|\varphi_C\rangle \simeq |0\rangle$. For times t such that $|B(t)| \simeq \pi/2 + 2\pi n$, $n \in \mathbb{N}$, the state $|\varphi_{AB}\rangle$ becomes maximally entangled. The origin of this entanglement can be heuristically explained by a simple argument: the ground state of the mechanical oscillator is a Gaussian wave packet in the position basis. Each possible position adds-up coherently introducing correlations in the lengths of the left and right cavities in Figure 1(a). This imprints correlations in the phases of the corresponding electromagnetic fields in modes A and B giving rise to entanglement. As long as the dimensionless optomechanical coupling k due to radiation pressure on the middle mirror is sufficiently small, mode C will be approximately unperturbed and therefore, to a good approximation, disentangled from AB . On the other hand, as the coupling strength increases mode C can become significantly entangled with modes A and B ; the entanglement of subsystems as a function of k will be addressed in the next section.

To quantitatively evaluate the entanglement in (5) we calculate the three-partite density matrix $\rho_{ABC} = |\Psi(t)\rangle\langle\Psi(t)|$, from which we obtain the reduced state $\rho_{AB} = \text{Tr}_C(\rho_{ABC})$:

$$\rho_{AB}(t) = \frac{1}{4} \begin{pmatrix} 1 & e^{C(t)} & e^{C(t)} & 1 \\ e^{C^*(t)} & 1 & e^{-2k^2|\eta(t)|^2} & e^{C^*(t)} \\ e^{C^*(t)} & e^{-2k^2|\eta(t)|^2} & 1 & e^{C^*(t)} \\ 1 & e^{C(t)} & e^{C(t)} & 1 \end{pmatrix} \quad (7)$$

with $C(t) = iB(t) - k^2|\eta(t)|^2/2$. Notice that for small values of k the mirror is “weakly entangled” with modes A and B and some of the off-diagonal terms of the reduced density matrix acquire exponentials that alternate between periods of decay and periods of growth. This can be seen as an example of a weak form of decoherence and “non-Markovian” evolution for the partitions of the whole system, in which information about the optical modes leak into correlations with the mirror and is later retrieved. The mirror introduces a “memory” in the system [43]. Non-Markovianity springs from the fact that the mirror is part of the system under study and hence its degrees of freedom are under control.

Since the state $\rho_{AB}(t)$ is restricted to the subspace spanned by $\{|0\rangle, |1\rangle\}$, we can use concurrence as a measure of entanglement. As an example, plots of the concurrence $\mathcal{C}_{AB}(t)$ and von Neumann entropy $S_{AB}(t)$ of ρ_{AB} are shown in Figure 2 for coupling value $k = 0.5$. The optical modes exhibit positive concurrence and hence entanglement as a function of time. Moreover, the system exhibits sudden death and birth of entanglement. It is also possible to see that the entropy, which is initially zero, oscillates as a function of time. This is another indication of the non-Markovian nature of the system. A non-zero entropy of AB signals entanglement among the three-partite system ABC . Moreover, note that the maxima of concurrence (entanglement of AB) coincide with the minima of entropy (entanglement of ABC). This suggests that entanglement “flows” (during the limited period of its lifetime) among different partitions of the system.

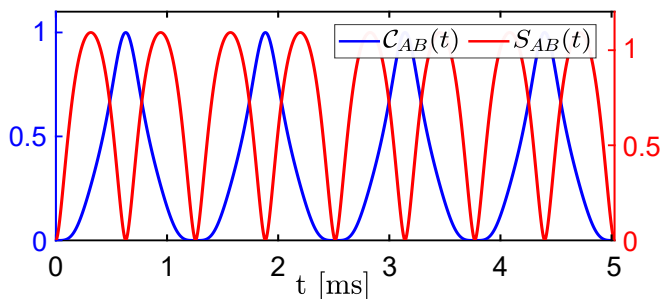


FIG. 2: Concurrence (blue) and von Neumann entropy (red) for $\rho_{AB}(t)$ as a function of time. For this plot $k = 0.5$.

Gaussian states — We now consider a scenario in which initially the optical modes are populated by monochromatic coherent states and the moving object (sphere, cloud of atoms or mirror) is in a thermal state at temperature T

$$\rho(0) = |\alpha\rangle\langle\alpha| \otimes |\beta\rangle\langle\beta| \otimes \frac{1}{Z} \sum_n e^{-\frac{n\hbar\omega_c}{k_B T}} |n\rangle\langle n|, \quad (8)$$

where $Z = \sum_n e^{-\frac{n\hbar\omega_c}{k_B T}}$ is the thermal partition function. Note $\rho(0)$ is a Gaussian separable state. Since the dynamical evolution (2) preserves Gaussianity [44], we can

conveniently use the Continuous Variable formalism to study the dynamics of entanglement and entropy of the subsystems through their time-dependent covariance matrices [44, 45] from which we can calculate exactly the logarithmic negativity, an entanglement monotone [46, 47], and the Von Neumann entropy. See Supplemental Material for an overview of the Continuous Variable formalism and details of the calculations.

Figure 3(a) shows an example of the logarithmic negativities and entropies for the different partitions of the system: AB (opto-opto), BC (opto-mechanical) and AC (opto-mechanical). Entanglement and entropy exhibit oscillations (death and revivals) of which one full period is shown. Note the initial decrease and subsequent increase in the entropies AC and BC , a characteristic of the non-Markovian nature of the system. As in the non-Gaussian case, the appearance of entanglement between optical modes, given the initially separable state, evidences the non-classicality of the mechanical mode [32].

We observe that the local maxima of logarithmic negativity for subsystems AC and BC coincide with local minima of the respective von Neumann entropies. At the same time, this reduction in entropy is accompanied by an increase in the entropy of modes AB . This suggests that as the entropy “leaks” from the mechanical oscillator into the optical modes, entanglement between modes AC and BC “builds up” and is later transferred to the optical modes. As in the non-Gaussian example, there seems to be evidence for the idea that entanglement flows among the various interacting subsystems. To firmly establish this idea, further investigation is necessary.

We note that the entanglement and entropy dynamics is strongly affected by the dimensionless optomechanical coupling k in a non-trivial way. This can be seen from the correlators of the system, e.g. equation (9), and from Figure 3(b) showing the maximum of the logarithmic negativity for the optical subsystem within one period τ as a function of the coupling k . See the Supplemental Material for further details.

$$\langle \hat{a}(t) \hat{b}(t)^\dagger \rangle = \alpha \beta^* e^{-i(r_a - r_b)t} e^{-|\beta|^2 [1 - e^{4iB(t)}]} e^{-|\alpha|^2 [1 - e^{-4iB(t)}]} e^{-k^2 |\eta(t)|^2 [4\bar{n} + 2]} \quad (9)$$

When $k < 1/\sqrt{2}$, the “low coupling” regime, the overall periodicity of the logarithmic negativities and von Neumann entropies is $\tau = \pi/\omega_m k^2$ and observation of entanglement revivals are only possible when $\pi/\omega_m k^2 \ll \kappa^{-1}$, where κ^{-1} is the inverse cavity linewidth, or the approximate photon lifetime in the cavity. This translates into the so-called photon blockade condition $g_0^2/(\omega_m \kappa) \gg 1$ [36, 48]. Furthermore, from Figure 3(b), we observe that $\max(\mathcal{E}_{AB})$ is mostly constant as a function of k . On the other hand, when $k \geq 1/\sqrt{2}$, “high coupling” regime, the periodicity is $\tau = 2\pi/\omega_m$ and observation

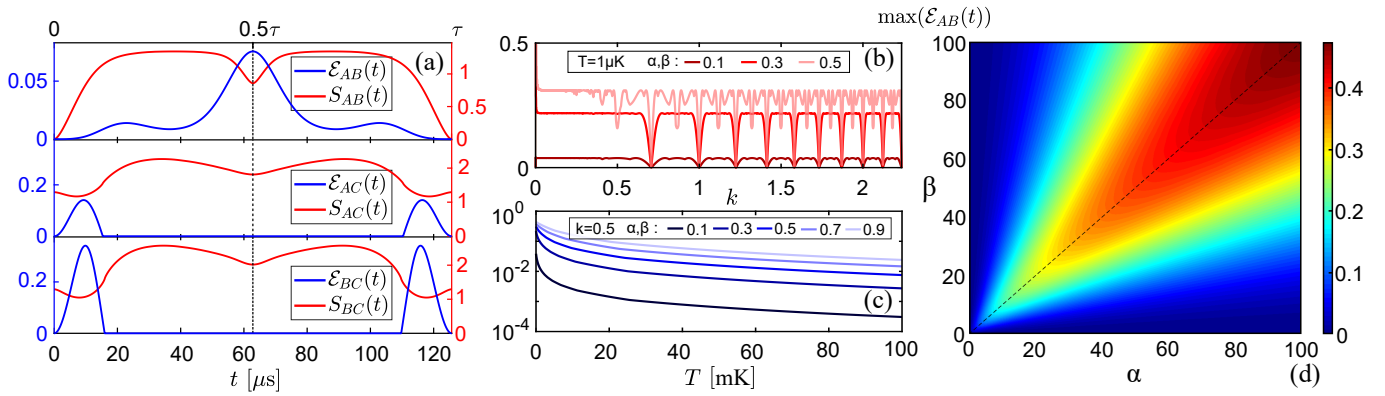


FIG. 3: **(a)** Entanglement as measured by the logarithmic negativity (blue) and the von Neumann entropies (red) for the various partitions of the system as a function of time. Different coherent state amplitudes of $\alpha = 0.5$ and $\beta = 0.7$ were chosen to exemplify the effect of asymmetrically populated optical modes. The remaining free parameters are chosen to be $k = 0.5$ and $T = 1 \mu\text{K}$. Maximum of the logarithmic negativity within one period τ for subsystem AB as function of **(b)** the dimensionless optomechanical coupling k , **(c)** the temperature T and **(d)** coherent state amplitudes α and β ; we assume, for simplicity, $\alpha = |\alpha|$ and $\beta = |\beta|$. We note the apparent peak near $k \sim 10^{-3}$ in (b). Due to the scaling of entanglement period with $1/k^2$, in this regime, the time necessary to observe entanglement blows up for small coupling values and computing $\max(\mathcal{E}_{AB})$ becomes numerically challenging. Since observing optical entanglement birth and death for small values of k is out of range from current experiments (see the Experimental Proposal section), we shall focus the discussion on values of $k > 10^{-3}$. For all three plots we used $\omega_a = \omega_b = 10^{15} \text{ Hz}$, $\omega_m = 10^5 \text{ Hz}$.

of entanglement dynamics is conditioned on satisfying $2\pi/\omega_m \ll \kappa^{-1}$. Moreover, $\max(\mathcal{E}_{AB})$ becomes very sensitive to small changes in k , presenting local minima at $2k^2 = N$, where $N \in \mathbb{N}^*$. Knowledge of this behavior can be used when designing an experiment for tailoring the entanglement properties of the system as desired. For instance, if optical entanglement is to be maximized, increasing coupling may not be the best strategy.

To characterise the effect of the oscillator's thermal fluctuations in the the optical entanglement we show a plot of $\max(\mathcal{E}_{AB})$ as a function of temperature in Figure 3(c). The entanglement persists well above the microkelvin temperatures reported in current optomechanical experiments [27, 49].

The mean number of photons in the cavity also plays an important role in optical entanglement generation. Figure 3(d) shows a surface plot of $\max(\mathcal{E}_{AB})$ as a function of the coherent state amplitudes α and β , taken to be real numbers for simplicity. We observe an increase in the maximal optical entanglement with mean photon numbers. There is, however, a trade-off: as the number of photons increase, the width of the peaks in $\mathcal{E}_{AB}(t)$ - and consequently the time during which entanglement is non-vanishing - decreases significantly, a feature which can also be qualitatively understood from the form of the correlators such as the one in (9). Moreover, it is also possible to see that entanglement is optimized when the energy is evenly distributed in the two optical modes, which happens when $\alpha = \beta$. Interestingly, as α and β increase the system becomes less sensitive to discrepancies between the mean photon numbers in each optical mode.

Experimental proposal — With increasing advances in the field of quantum cavity optomechanics [49–51] experiments in the high coupling and long coherence time regimes are expected. However, most current optomechanical systems have small coupling values and observing entanglement dynamics as described in the present work remains challenging. One notable exception and a promising candidate set-up is optomechanics with ultracold atomic ensembles where a coherent cloud of atoms is trapped within an optical cavity and the collective center of mass coordinate effectively behaves as a quantum mechanical oscillator. Couplings as high as $k \approx 10$ have been reported in such ultracold experiments [27], and the system allows wide tunability of the relevant parameters.

TABLE I: Proposed values for the experimental implementation with ultracold atoms.

Parameter	Units	Value
Number of atoms	-	5.43×10^5
Trap frequency ω_m	kHz	600
Coupling $k = \frac{g_0}{\omega_m}$	-	0.74
Mechanical dissipation $\Gamma/2\pi$	kHz	1
Cavity Finesse \mathcal{F}	-	3×10^6
Cavity Length L	μm	783
Cavity Linewidth κ	kHz	64
Temperature T	μK	0.8
Mean photon number $ \alpha ^2 = \beta ^2$	-	0.25

To observe entanglement dynamics the lifetime of a photon inside the cavity $1/\kappa$ needs to be longer than the

‘entangling time’, the time at which optical entanglement reaches its first local maximum. Table I presents values for the relevant experimental parameters adapted from [27]. With these numbers the resulting cavity photon lifetime is 15.7×10^{-6} s while the entangling period is 10.5×10^{-6} s. The corresponding negativity was found to be $\max(\mathcal{E}_{AB}) \approx 0.3$. This suggests that in these systems the observation of dispersive mechanically-induced optical entanglement could be within reach.

Conclusion — In this Letter we have studied the entanglement and entropy dynamics of a “mirror-in-the-middle” optomechanical system. Implementations using levitated particles have been briefly discussed. We have seen that an initially separable state can evolve to an entangled wavefunction, exhibiting birth and death of entanglement and entropy both for non-Gaussian and Gaussian states. The appearance of entanglement in this setting evidences the non-classical nature of the mechanical oscillator.

The entanglement dynamics is strongly influenced by the system parameters, notably the optomechanical coupling $k = g_0/\omega_m$ and the mean number of photons in the experiment. We have shown the existence of two distinct regimes depending on whether $k < 1/\sqrt{2}$ or $k \geq 1/\sqrt{2}$. In addition, we have observed that optical entanglement is maximized when the energy is evenly distributed in the optical modes and that it persists well above microkelvin temperatures of the mechanical mode. This is valuable information when designing an experiment. Optomechanics with ultracold atomic ensembles presents an interesting candidate for implementing the studied entanglement dynamics.

Although a promising candidate, the dispersive Hamiltonian is not the only available platform to untangle the dynamics of entanglement and information flow in optomechanical systems. Exploring alternatives such as coherent scattering [52–54] might prove to be a very fruitful approach to observe entanglement and non-classicality in experimental optomechanical systems.

Acknowledgments — This work was financed in part by the Serrapilheira Institute (grant number Serra-1709-21072), by Coordenação de Aperfeiçoamento de Pessoal de Nível Superior - Brasil (CAPES) - Finance Code 001 and by Conselho Nacional de Desenvolvimento Científico e Tecnológico (CNPq). I. B. thanks the support received by the FAPERJ Scholarship No. E-26/200.270/2020. T.G. thanks the support received by the FAPERJ Scholarship No. E-26/202.830/2019.

* igorbrandao@aluno.puc-rio.br

† bruno.b.suassuna@gmail.com

‡ brunomelo@aluno.puc-rio.br

§ barbosa@puc-rio.br

- [1] E. Schrodinger. Die gegenwärtige situation in der quantenmechanik. *Die Naturwissenschaften*, 23(48):807–812, nov 1935.
- [2] V. Vedral. Quantifying entanglement in macroscopic systems. *Nature*, 453(7198):1004–1007, jun 2008.
- [3] J. Preskill. Quantum Computing in the NISQ era and beyond. *Quantum*, 2:79, August 2018.
- [4] R. P. Feynman. *Feynman lectures on gravitation*. 12 1996.
- [5] L. Diósi. A universal master equation for the gravitational violation of quantum mechanics. *Physics Letters A*, 120(8):377–381, mar 1987.
- [6] R. Penrose. On gravity’s role in quantum state reduction. *General Relativity and Gravitation*, 28(5):581–600, may 1996.
- [7] S. Bose, A. Mazumdar, G. W. Morley, H. Ulbricht, M. Toroš, M. Paternostro, A. A. Geraci, P. F. Barker, M. S. Kim, and G. Milburn. Spin entanglement witness for quantum gravity. *Phys. Rev. Lett.*, 119:240401, Dec 2017.
- [8] M. P. Blencowe. Effective field theory approach to gravitationally induced decoherence. *Phys. Rev. Lett.*, 111:021302, Jul 2013.
- [9] I. Pikovski, M. Zych, F. Costa, and Č. Brukner. Universal decoherence due to gravitational time dilation. *Nature Physics*, 11(8):668–672, jun 2015.
- [10] A. Belenchia, R. M. Wald, F. Giacomini, E. Castro-Ruiz, Č. Brukner, and M. Aspelmeyer. Information content of the gravitational field of a quantum superposition. *International Journal of Modern Physics D*, 28(14):1943001, oct 2019.
- [11] D. Carney, P. C. E. Stamp, and J. M. Taylor. Table-top experiments for quantum gravity: a user’s manual. *Classical and Quantum Gravity*, 36(3):034001, jan 2019.
- [12] Ryan J. Marshman, Anupam Mazumdar, and Sougato Bose. Locality and entanglement in table-top testing of the quantum nature of linearized gravity. *Physical Review A*, 101(5), may 2020.
- [13] M. Aspelmeyer, T. J. Kippenberg, and F. Marquardt. Cavity optomechanics. *Rev. Mod. Phys.*, 86:1391–1452, Dec 2014.
- [14] S. Mancini, V. I. Man’ko, and P. Tombesi. Ponderomotive control of quantum macroscopic coherence. *Phys. Rev. A*, 55:3042–3050, Apr 1997.
- [15] V. Giovannetti, S. Mancini, and P. Tombesi. Radiation pressure induced einstein-podolsky-rosen paradox. *Europhysics Letters (EPL)*, 54(5):559–565, jun 2001.
- [16] S. Bose, K. Jacobs, and P. L. Knight. Preparation of nonclassical states in cavities with a moving mirror. *Phys. Rev. A*, 56:4175–4186, Nov 1997.
- [17] S. Mancini, V. Giovannetti, D. Vitali, and P. Tombesi. Entangling macroscopic oscillators exploiting radiation pressure. *Phys. Rev. Lett.*, 88:120401, Mar 2002.
- [18] J. Zhang, K. Peng, and S. L. Braunstein. Quantum-state transfer from light to macroscopic oscillators. *Phys. Rev. A*, 68:013808, Jul 2003.
- [19] S. Pirandola, D. Vitali, P. Tombesi, and S. Lloyd. Macroscopic entanglement by entanglement swapping. *Phys. Rev. Lett.*, 97:150403, Oct 2006.
- [20] T. Corbitt, Y. Chen, F. Khalili, D. Ottaway, S. Vyatchanin, S. Whitcomb, and N. Mavalvala. Squeezed-state source using radiation-pressure-induced rigidity. *Phys. Rev. A*, 73:023801, Feb 2006.

- [21] C. Wipf, T. Corbitt, Y. Chen, and N. Mavalvala. Route to ponderomotive entanglement of light via optically trapped mirrors. *New Journal of Physics*, 10(9):095017, sep 2008.
- [22] Xin-You Lü, Jie-Qiao Liao, L. Tian, and F. Nori. Steady-state mechanical squeezing in an optomechanical system via duffing nonlinearity. *Physical Review A*, 91(1), jan 2015.
- [23] D. W. C. Brooks, T. Botter, S. Schreppler, T. P. Purdy, N. Brahms, and D. M. Stamper-Kurn. Non-classical light generated by quantum-noise-driven cavity optomechanics. *Nature*, 488(7412):476–480, aug 2012.
- [24] T. P. Purdy, P.-L. Yu, R. W. Peterson, N. S. Kampel, and C. A. Regal. Strong optomechanical squeezing of light. *Phys. Rev. X*, 3:031012, Sep 2013.
- [25] N. Aggarwal, T. Cullen, J. Cripe, G. D. Cole, R. Lanza, A. Libson, D. Follman, P. Heu, T. Corbitt, and N. Mavalvala. Room temperature optomechanical squeezing. arXiv: 1812.09942v1.
- [26] J. Chen, M. Rossi, D. Mason, and A. Schliesser. Entanglement of propagating optical modes via a mechanical interface. *Nature Communications*, 11(1), feb 2020.
- [27] K. W. Murch, K. L. Moore, S. Gupta, and D. M. Stamper-Kurn. Observation of quantum-measurement backaction with an ultracold atomic gas. *Nature Physics*, 4(7):561–564, may 2008.
- [28] A. M. Jayich, J. C. Sankey, B. M. Zwickl, C. Yang, J. D. Thompson, S. M. Girvin, A. A. Clerk, F. Marquardt, and J. G. E. Harris. Dispersive optomechanics: a membrane inside a cavity. *New Journal of Physics*, 10(9):095008, sep 2008.
- [29] A. H. Safavi-Naeini, S. Grblacher, J. T. Hill, J. Chan, M. Aspelmeyer, and O. Painter. Squeezed light from a silicon micromechanical resonator. *Nature*, 500(7461):185–189, aug 2013.
- [30] T. Krisnanda, M. Zuppardo, M. Paternostro, and T. Paterek. Revealing nonclassicality of inaccessible objects. *Phys. Rev. Lett.*, 119:120402, Sep 2017.
- [31] Yue Ma, Federico Armata, Kiran E. Khosla, and M. S. Kim. Optical squeezing for an optomechanical system without quantizing the mechanical motion. *Physical Review Research*, 2(2), may 2020.
- [32] C. Marletto and V. Vedral. Gravitationally induced entanglement between two massive particles is sufficient evidence of quantum effects in gravity. *Phys. Rev. Lett.*, 119:240402, Dec 2017.
- [33] D. E. Chang, C. A. Regal, S. B. Papp, D. J. Wilson, J. Ye, O. Painter, H. J. Kimble, and P. Zoller. Cavity opto-mechanics using an optically levitated nanosphere. *Proceedings of the National Academy of Sciences*, 107(3):1005–1010, dec 2009.
- [34] O. Romero-Isart, M. L. Juan, R. Quidant, and J. I. Cirac. Toward quantum superposition of living organisms. *New Journal of Physics*, 12(3):033015, mar 2010.
- [35] N. Kiesel, F. Blaser, U. Delić, D. Grass, R. Kaltenbaek, and M. Aspelmeyer. Cavity cooling of an optically levitated submicron particle. *Proceedings of the National Academy of Sciences*, 110(35):14180–14185, 2013.
- [36] L. Neumeier, T. E. Northup, and D. E. Chang. Reaching the optomechanical strong-coupling regime with a single atom in a cavity. *Physical Review A*, 97(6), jun 2018.
- [37] F. Brennecke, S. Ritter, T. Donner, and T. Esslinger. Cavity optomechanics with a bose-einstein condensate. *Science*, 322(5899):235–238, oct 2008.
- [38] M. Takatsuji. Quantum theory of the optical kerr effect. *Phys. Rev.*, 155:980–986, Mar 1967.
- [39] E. Lombardi, F. Sciarrino, S. Popescu, and F. De Martini. Teleportation of a vacuum–one-photon qubit. *Physical Review Letters*, 88(7), jan 2002.
- [40] T. Guerreiro, F. Monteiro, A. Martin, J. B. Brask, T. Vértesi, B. Korzh, M. Caloz, F. Bussiès, V. B. Verma, A. E. Lita, R. P. Mirin, S. W. Nam, F. Marsilli, M. D. Shaw, N. Gisin, N. Brunner, H. Zbinden, and R. T. Thew. Demonstration of einstein-podolsky-rosen steering using single-photon path entanglement and displacement-based detection. *Physical Review Letters*, 117(7), aug 2016.
- [41] T. Peyronel, O. Firstenberg, Qi-Yu Liang, S. Hofferberth, A. V. Gorshkov, T. Pohl, M. D. Lukin, and V. Vuletić. Quantum nonlinear optics with single photons enabled by strongly interacting atoms. *Nature*, 488(7409):57–60, jul 2012.
- [42] M. Hofheinz, H. Wang, M. Ansmann, R. C. Bialczak, E. Lucero, M. Neeley, A. D. O’Connell, D. Sank, J. Wenner, J. M. Martinis, and A. N. Cleland. Synthesizing arbitrary quantum states in a superconducting resonator. *Nature*, 459(7246):546–549, may 2009.
- [43] Heinz-Peter Breuer and F. Petruccione. *The Theory of Open Quantum Systems*. Oxford University Press, 2007.
- [44] C. Weedbrook, S. Pirandola, R. García-Patrón, N. J. Cerf, T. C. Ralph, J. H. Shapiro, and S. Lloyd. Gaussian quantum information. *Rev. Mod. Phys.*, 84:621–669, May 2012.
- [45] J. Laurat, G. Keller, J. A. Oliveira-Huguenin, C. Fabre, T. Coudreau, A. Serafini, G. Adesso, and F. Illuminati. Entanglement of two-mode gaussian states: characterization and experimental production and manipulation. *Journal of Optics B: Quantum and Semiclassical Optics*, 7(12):S577–S587, nov 2005.
- [46] G. Vidal and R. F. Werner. Computable measure of entanglement. *Phys. Rev. A*, 65:032314, Feb 2002.
- [47] M. B. Plenio. Logarithmic negativity: A full entanglement monotone that is not convex. *Phys. Rev. Lett.*, 95:090503, Aug 2005.
- [48] P. Rabl. Photon blockade effect in optomechanical systems. *Phys. Rev. Lett.*, 107:063601, Aug 2011.
- [49] Uroš Delić, Manuel Reisenbauer, Kahan Dare, David Grass, Vladan Vuletić, Nikolai Kiesel, and Markus Aspelmeyer. Cooling of a levitated nanoparticle to the motional quantum ground state. *Science*, 367(6480):892–895, jan 2020.
- [50] D. Windey, C. Gonzalez-Ballester, P. Maurer, L. Novotny, O. Romero-Isart, and R. Reimann. Cavity-based 3d cooling of a levitated nanoparticle via coherent scattering. *Physical Review Letters*, 122(12), mar 2019.
- [51] A. de los Ros Sommer, N. Meyer, and R. Quidant. Strong optomechanical coupling at room temperature by coherent scattering. arXiv: 2005.10201v1.
- [52] Henning Rudolph, Klaus Hornberger, and Benjamin A. Stickler. Entangling levitated nanoparticles by coherent scattering. *Physical Review A*, 101(1), jan 2020.
- [53] Anil Kumar Chauhan, Ondřej Černotík, and Radim Filip. Stationary gaussian entanglement between levitated nanoparticles.
- [54] Ondřej Černotík and Radim Filip. Strong mechanical squeezing for a levitated particle by coherent scattering. *Physical Review Research*, 2(1), jan 2020.

- [55] Jan Gieseler, Bradley Deutsch, Romain Quidant, and Lukas Novotny. Subkelvin parametric feedback cooling of a laser-trapped nanoparticle. *Physical Review Letters*, 109(10), sep 2012.
- [56] Gerard P. Conangla, Francesco Ricci, Marc T. Cuairan, Andreas W. Schell, Nadine Meyer, and Romain Quidant. Optimal feedback cooling of a charged levitated nanoparticle with adaptive control. *Physical Review Letters*, 122(22), jun 2019.
- [57] Nadine Meyer, Andrés de los Rios Sommer, Pau Mestres, Jan Gieseler, Vijay Jain, Lukas Novotny, and Romain Quidant. Resolved-sideband cooling of a levitated nanoparticle in the presence of laser phase noise. *Physical Review Letters*, 123(15), oct 2019.
- [58] U. Delić, M. Reisenbauer, D. Grass, N. Kiesel, V. Vuletić, and M. Aspelmeyer. Cavity cooling of a levitated nanosphere by coherent scattering. *Physical Review Letters*, 122(12), mar 2019.

Supplemental Material

I. IMPLEMENTATION USING LEVITATED NANOPARTICLES

Consider the system shown in Figure S1: a nanoparticle of radius r , mass m and refractive index n_p is trapped in an harmonic trap of frequencies $\omega_{j=x,y,z}$ created by an optical tweezer inside a cavity populated by two optical modes of frequencies ω_a and ω_b and annihilation/creation operators \hat{a}/\hat{a}^\dagger and \hat{b}/\hat{b}^\dagger , respectively. The presence of the particle causes a position dependent shift on the cavity's resonance frequencies, so that the Hamiltonian of this system becomes [35]

$$\frac{\hat{H}}{\hbar} = \omega_a \hat{a}^\dagger \hat{a} - U_{0,a} \sin^2[k_a(x_0 + x)] \hat{a}^\dagger \hat{a} + \omega_b \hat{b}^\dagger \hat{b} - U_{0,b} \sin^2[k_b(x_0 + x)] \hat{b}^\dagger \hat{b} + \sum_{j=x,y,z} \omega_j \hat{c}_j^\dagger \hat{c}_j, \quad (\text{S1})$$

where x_0 is the position of the center of the trap, x is the particle's displacement, $U_{0,i} = \omega \hat{a}_i \alpha / 2\epsilon_0 V_i$ is the frequency shift when the particle is at an intensity maximum of the cavity, $\alpha = 4\pi\epsilon_0 r^3(n_p^2 - 1)/(n_p^2 + 2)$ is the polarizability of the particle, V_i and k_i are the volume and the wavenumber of mode i , respectively, and $\hat{c}_j/\hat{c}_j^\dagger$ is the phonon annihilation/creation operators along axis $j = x, y, z$. We will not consider driving terms since we are interested in the dynamics of an isolated cavity without the influence of external systems such as a driving laser, as explained in the main text.

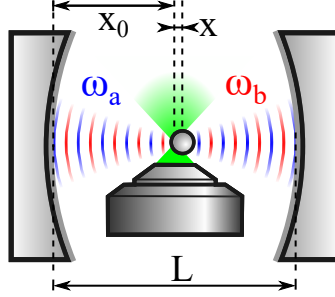


FIG. S1: A nanoparticle, trapped by an optical tweezer, is placed along the axis of a cavity populated by two optical modes of frequencies ω_a and ω_b . If the position x_0 of the center of the optical trap is properly chosen, the coupling between particle and light becomes linear on the particle's displacement.

The interaction terms may yield linear couplings between the optical modes and the sphere if x_0 , k_a and k_b are properly chosen. Expanding $\sin^2 k_i(x_0 + x)$ around x_0 gives

$$\sin^2 k_i(x_0 + x) = \sin^2 k_i x_0 + k_a \sin(2k_a x_0)x + 2k_a^2 \cos(2k_a x_0)x^2 + \mathcal{O}(x^3). \quad (\text{S2})$$

Now, consider the particular case in which the frequencies of the optical modes are two consecutive resonance frequencies, and let $L = 2n(\lambda_a/2) = (2n+1)(\lambda_b/2)$ without loss of generality. Then, if the sphere is placed near the center of the cavity at $x_0 = L/2 + \lambda_a/8 \approx L/2 + \lambda_b/8$, we have

$$\sin^2 k_a(x_0 + x) \approx 1/2 + k_a x \quad (\text{S3})$$

and

$$\sin^2 k_b(x_0 + x) \approx 1/2 - k_b x. \quad (\text{S4})$$

Substituting these approximations in equation (S1) and disregarding the motion along the y and z axes, we get

$$\frac{\hat{H}}{\hbar} = \omega'_a \hat{a}^\dagger \hat{a} - g_0 \hat{a}^\dagger \hat{a} (\hat{c}_x^\dagger + \hat{c}_x) + \omega'_b \hat{b}^\dagger \hat{b} + g_0 \hat{b}^\dagger \hat{b} (\hat{c}_x^\dagger + \hat{c}_x) + \omega_x \hat{c}_x^\dagger \hat{c}_x,$$

where $\omega'_a = \omega_a - U_{0,a}/2$ and $g_0 = U_{0,a} k_a x_{ZPF} \approx U_{0,b} k_b x_{ZPF}$ is the intended linear coupling, with $x_{ZPF} = \sqrt{\hbar/2m\omega_x}$ the zero-point fluctuation. This Hamiltonian is formally equivalent to that of a double-sided cavity with a moving “mirror-in-the-middle” analysed in the main text, with the condition $g_{0,a} \approx g_{0,b}$ being met due to the use of consecutive

resonance frequencies. As a final remark, note that the modes A and B are not used for cooling of the particle, which is necessary for observing optical entanglement in the system [32]. Cooling of the center-of-mass motion of the particle can be addressed in a number of ways, such as a feedback acting on the trapping laser [55, 56], dispersive coupling with a third optical mode [57] or coherent scattering between the trapping beam and the optical cavity [50, 51, 58].

II. IMPLEMENTATION USING ULTRACOLD ATOMIC ENSEMBLES

In ultracold atom optomechanical experiments, an atomic ensemble is trapped inside an optical cavity. Collective center-of-mass motion of the atoms alters the cavity resonance frequency. It is similar to the dispersive optomechanical experiments with levitated spheres described in the previous section, with the cloud of atoms playing the role of levitated nanoparticle.

The optomechanical coupling between an ultracold atomic cloud and a cavity optical mode with wavelength λ_a is [27]

$$g_{0,a} = k_a N \frac{\alpha_0^2}{\Delta_{ca}} \sin(2k_a z_0) \sqrt{\frac{\hbar}{2Nm\omega_m}}, \quad (\text{S5})$$

where k_a is the wavenumber, N is the number of atoms, Δ_{ca} is the atom-cavity detuning, m is the mass of a single atom, ω_m is the mechanical frequency and $\alpha_0 = \sqrt{d^2\omega_c/2\hbar\epsilon_0 V_c}$ is the atom-single photon coupling rate, with d the dipole moment for the transition between the relevant atomic levels and V_c the cavity volume. Reported values from Ref. [27] for these quantities are shown in Table S1. As in the previous case of a levitated nanoparticle, we chose $\sin(2k_a z_0) = 1$. The wavelength λ_b should be chosen so that $\sin(2k_b z_0) = -1$, as to provide $g_{0,a} = g_{0,b}$.

TABLE S1: Values reported in [27].

Parameter	Units	Value
Number of atoms	-	10^5
Trap frequency ω_m	kHz	$2\pi \times 40$
Coupling $k = \frac{g_0}{\omega_m}$	-	9.50
Cavity Finesse \mathcal{F}	-	5.8×10^5
Cavity Length L	μm	194
Cavity mirror's radius R	cm	5
Cavity Linewidth κ	MHz	$2\pi \times 0.66$
Temperature T	μK	0.8

As discussed in the main text, for the entanglement dynamics experiment to be feasible, the photon-lifetime τ_p must be greater than the entanglement period τ_e . One of the main constraints in fulfilling this condition is set by the Finesse of the cavity. Therefore, we look for the minimum value of τ_e/τ_p by varying the cavity length L , the number of atoms N and the mechanical frequency ω_m around the values in Table S1, and then calculate the minimum Finesse necessary to make $\tau_e/\tau_p < 1$ given the optimal values of L , N and ω_m .

In doing these calculations, it is necessary to account for the changes in the mode volume, given by $V_c = \pi w_a^2 L$, where

$$w_a = \sqrt{\frac{\lambda_a}{2\pi}} \sqrt{L(2R - L)} \quad (\text{S6})$$

is the mode's waist, and the changes in the cavity linewidth

$$\kappa = \frac{\mathcal{F}}{\nu_{FSR}} \quad (\text{S7})$$

with $\nu_{FSR} = c/2L$ the cavity's free spectral range. Finally, it is important to make sure that $k = g_0/\omega_m \neq \sqrt{N/2}$, $N \in \mathbb{N}^*$, since the maximum of logarithmic negativity is significantly smaller for these coupling values. We find that for $L = 783 \mu\text{m}$, $N = 5.43 \times 10^5$ and $\omega_m = 2\pi \times 95 \text{ kHz}$ the dimensionless optomechanical coupling is $k = 0.743$ and the entanglement period to photon lifetime ratio is $\tau_e/\tau_p = 3.46$. The Finesse should then be increased to 2.01×10^6 ,

so that $\tau_e/\tau_p \simeq 1$ and entanglement becomes measurable. In the main text, the proposed Finesse is about 1.5 times larger, so that $\tau_e/\tau_p = 0.669$.

Another parameter that could be varied are the radii of the cavity mirrors. Considering 1 cm, 2.5 cm, 5 cm and 10 cm as possible radii, we find the values presented in Table S2. As we can see, the Finesse constraint can be relaxed provided that a smaller radius is used. Overall, the necessary values for N , ω_m and \mathcal{F} differ by less than one order of magnitude from reported values in the literature.

TABLE S2: Optimal parameters for different cavity mirror's radii.

R(cm)	$L(\mu\text{m})$	$N(10^5)$	$\omega_m(\text{kHz})$	$\mathcal{F}(10^6)$
1	1211	3.85	$2\pi \times 95$	1.30
2.5	1035	5.64	$2\pi \times 92$	1.57
5	783	5.43	$2\pi \times 95$	2.01
10	669	5.80	$2\pi \times 91$	2.47

III. THE UNITARY EVOLUTION

The “mirror-in-the-middle” Hamiltonian can be written as

$$\frac{\hat{H}}{\hbar} = \omega_m \hat{c}^\dagger \hat{c} + \omega_a \hat{a}^\dagger \hat{a} + \omega_b \hat{b}^\dagger \hat{b} - g_0 (\hat{a}^\dagger \hat{a} - \hat{b}^\dagger \hat{b}) (\hat{c} + \hat{c}^\dagger), \quad (\text{S8})$$

where \hat{a} , \hat{b} and \hat{c} denote annihilation operators for the optical mode in the left cavity (A), right cavity (B) and the mechanical oscillator (C), respectively. In what follows we will work with the re-scaled time $\omega_m t$, denoted henceforth by t , and introduce the dimensionless variables $r_a = \omega_a/\omega_m$, $r_b = \omega_b/\omega_m$ and $k = g_0/\omega_m$.

Define the unitary operator [16]

$$\hat{E}(k) = \exp\left(k(\hat{a}^\dagger \hat{a} - \hat{b}^\dagger \hat{b})(\hat{c}^\dagger - \hat{c})\right). \quad (\text{S9})$$

The operator $\hat{E}(k)$ commutes with $\hat{a}^\dagger \hat{a}$ and $\hat{b}^\dagger \hat{b}$, but not with \hat{c} ,

$$\hat{E}(k)^\dagger \hat{c} \hat{E}(k) = \hat{c} + k(\hat{a}^\dagger \hat{a} - \hat{b}^\dagger \hat{b}), \quad (\text{S10})$$

which is calculated through the general identity,

$$e^{-\hat{A}} \hat{B} e^{+\hat{A}} = \hat{B} + [\hat{B}, \hat{A}] + \frac{1}{2}[\hat{B}, \hat{A}]^2 + \frac{1}{3!}[[\hat{B}, \hat{A}], \hat{A}] + \dots \quad (\text{S11})$$

Using equation (S10) and its adjoint, we have

$$\hat{E}(k)^\dagger \frac{\hat{H}}{\hbar \omega_m} \hat{E}(k) = \hat{c}^\dagger \hat{c} + r_a \hat{a}^\dagger \hat{a} + r_b \hat{b}^\dagger \hat{b} - k^2 (\hat{a}^\dagger \hat{a} - \hat{b}^\dagger \hat{b})^2. \quad (\text{S12})$$

Considering the number basis $\{|n, m, \ell\rangle\}$, we see by the equation above that $\hat{E}(k)|n, m, \ell\rangle$ are the energy eigenstates of the system. Those are of the form:

$$\hat{E}(k)|n, m, \ell\rangle = \hat{\mathcal{D}}_C(k(n-m))|n, m, \ell\rangle, \quad (\text{S13})$$

where we denote the displacement operator of the mechanical oscillator by $\hat{\mathcal{D}}_C(\kappa) = \exp(\kappa \hat{c}^\dagger - \kappa^* \hat{c})$, where κ is a complex number. The energies corresponding to the eigenstates above are

$$E_{n,m,\ell} = \hbar \omega_m \ell + \hbar \omega_a n + \hbar \omega_b m - \hbar \omega_m k^2 (n-m)^2. \quad (\text{S14})$$

By exponentiation of equation (S12), the unitary evolution operator is found to be

$$\hat{U}(t) = \hat{E}(k) e^{-i(\hat{c}^\dagger \hat{c} + r_a \hat{a}^\dagger \hat{a} + r_b \hat{b}^\dagger \hat{b} - k^2 (\hat{a}^\dagger \hat{a} - \hat{b}^\dagger \hat{b})^2) t} \hat{E}(k)^\dagger. \quad (\text{S15})$$

Next, we recall that $e^{i\hat{c}^\dagger \hat{c} t} \hat{c}^\dagger e^{-i\hat{c}^\dagger \hat{c} t} = e^{it} \hat{c}^\dagger$ and $e^{i\hat{c}^\dagger \hat{c} t} \hat{c} e^{-i\hat{c}^\dagger \hat{c} t} = e^{-it} \hat{c}$, from which we derive the following identity

$$e^{i\hat{c}^\dagger \hat{c} t} \hat{A}(\hat{c}^\dagger - \hat{c}) e^{-i\hat{c}^\dagger \hat{c} t} = \hat{A}(e^{it} \hat{c}^\dagger - e^{-it} \hat{c}) \Rightarrow e^{i\hat{c}^\dagger \hat{c} t} e^{\hat{A}(\hat{c}^\dagger - \hat{c})} e^{-i\hat{c}^\dagger \hat{c} t} = e^{\hat{A}(e^{it} \hat{c}^\dagger - e^{-it} \hat{c})}, \quad (\text{S16})$$

where \hat{A} is an operator that commutes with both \hat{c} and \hat{c}^\dagger .

Letting $\hat{A} = k(\hat{a}^\dagger \hat{a} - \hat{b}^\dagger \hat{b})$ in the identity above, we conclude that

$$\hat{E}(k) e^{-i\hat{c}^\dagger \hat{c} t} = e^{-i\hat{c}^\dagger \hat{c} t} e^{i\hat{c}^\dagger \hat{c} t} \hat{E}(k) e^{-i\hat{c}^\dagger \hat{c} t} = e^{-i\hat{c}^\dagger \hat{c} t} \exp\left(k(\hat{a}^\dagger \hat{a} - \hat{b}^\dagger \hat{b})(\hat{c}^\dagger e^{it} - \hat{c} e^{-it})\right), \quad (\text{S17})$$

hence,

$$\hat{E}(k) e^{-i\hat{c}^\dagger \hat{c} t} \hat{E}(k)^\dagger = e^{-i\hat{c}^\dagger \hat{c} t} \exp\left(k(\hat{a}^\dagger \hat{a} - \hat{b}^\dagger \hat{b})(\hat{c}^\dagger e^{it} - \hat{c} e^{-it})\right) \exp\left(k(\hat{a}^\dagger \hat{a} - \hat{b}^\dagger \hat{b})(\hat{c}^\dagger - \hat{c})\right). \quad (\text{S18})$$

We note the commutator

$$\frac{1}{2}[\hat{c}^\dagger e^{it} - \hat{c} e^{-it}, \hat{c}^\dagger - \hat{c}] = i \sin(t), \quad (\text{S19})$$

with which it becomes straightforward to compute

$$\frac{1}{2}[k(\hat{a}^\dagger \hat{a} - \hat{b}^\dagger \hat{b})(\hat{c}^\dagger e^{it} - \hat{c} e^{-it}), k(\hat{a}^\dagger \hat{a} - \hat{b}^\dagger \hat{b})(\hat{c}^\dagger - \hat{c})] = ik^2(\hat{a}^\dagger \hat{a} - \hat{b}^\dagger \hat{b})^2 \sin(t). \quad (\text{S20})$$

Since this commutes with both $(\hat{a}^\dagger \hat{a} - \hat{b}^\dagger \hat{b})(\hat{c}^\dagger e^{it} - \hat{c} e^{-it})$ and $(\hat{a}^\dagger \hat{a} - \hat{b}^\dagger \hat{b})(\hat{c}^\dagger - \hat{c})$, equation (S18) can be simplified using the particular form of the Baker-Campbell-Hausdorff formula

$$e^{\hat{A}} e^{\hat{B}} = e^{\hat{A} + \hat{B} + \frac{1}{2}[\hat{A}, \hat{B}]}, \quad (\text{S21})$$

valid when operators \hat{A} and \hat{B} commute with $[\hat{A}, \hat{B}]$. Thus, the expression

$$\hat{U}(t) = e^{-i\hat{c}^\dagger \hat{c} t} e^{-ir_a \hat{a}^\dagger \hat{a} t} e^{-ir_b \hat{b}^\dagger \hat{b} t} e^{k(\hat{a}^\dagger \hat{a} - \hat{b}^\dagger \hat{b})(\hat{c} \eta(t) - \hat{c}^\dagger \eta(t)^*)} e^{-i(\hat{a}^\dagger \hat{a} - \hat{b}^\dagger \hat{b})^2 B(t)} \quad (\text{S22})$$

holds for the unitary evolution operator $\hat{U}(t)$, where $\eta(t) = 1 - e^{-it}$ and $B(t) = -k^2(t - \sin(t))$.

In the interaction picture, we evolve states according to

$$\hat{U}_{\text{I.P.}}(t) = e^{k(\hat{a}^\dagger \hat{a} - \hat{b}^\dagger \hat{b})(\hat{c} \eta(t) - \hat{c}^\dagger \eta(t)^*)} e^{-i(\hat{a}^\dagger \hat{a} - \hat{b}^\dagger \hat{b})^2 B(t)}. \quad (\text{S23})$$

The Heisenberg evolution of the annihilation operators \hat{a} , \hat{b} and \hat{c} can then be derived,

$$\hat{a}(t) = U^\dagger(t) \hat{a} \hat{U}(t) = e^{-i(r_a t + B(t))} e^{2iB(t) \hat{b}^\dagger \hat{b}} e^{-2iB(t) \hat{a}^\dagger \hat{a}} \hat{\mathcal{D}}_C(\kappa)(+k\xi(t)) \hat{a}, \quad (\text{S24})$$

$$\hat{b}(t) = U^\dagger(t) \hat{b} \hat{U}(t) = e^{-i(r_b t + B(t))} e^{-2iB(t) \hat{b}^\dagger \hat{b}} e^{2iB(t) \hat{a}^\dagger \hat{a}} \hat{\mathcal{D}}_C(\kappa)(-k\xi(t)) \hat{b}, \quad (\text{S25})$$

$$\hat{c}(t) = U^\dagger(t) \hat{c} \hat{U}(t) = \hat{c} e^{-it} + k(\hat{a}^\dagger \hat{a} - \hat{b}^\dagger \hat{b}) \eta(t), \quad (\text{S26})$$

where $\xi(t) = e^{it} \eta(t) = e^{it} - 1 = -\eta(t)^*$. In deriving these expressions we made use of the relations

$$e^{i\hat{A}\hat{a}^\dagger \hat{a}} \hat{a} e^{-i\hat{A}\hat{a}^\dagger \hat{a}} = e^{-i\hat{A}} \hat{a}, \quad (\text{S27})$$

$$e^{i\hat{A}(\hat{a}^\dagger \hat{a})^2} \hat{a} e^{-i\hat{A}(\hat{a}^\dagger \hat{a})^2} = e^{-i\hat{A}(2\hat{a}^\dagger \hat{a} + I)} \hat{a}, \quad (\text{S28})$$

applicable whenever \hat{A} commutes with both \hat{a} and \hat{a}^\dagger . For instance, equation (S26) is derived as

$$\begin{aligned} U^\dagger(t) \hat{c} \hat{U}(t) &= e^{-k(\hat{a}^\dagger \hat{a} - \hat{b}^\dagger \hat{b})(\hat{c} \eta(t) - \hat{c}^\dagger \eta(t)^*)} e^{+i\hat{c}^\dagger \hat{c} t} \hat{c} e^{-i\hat{c}^\dagger \hat{c} t} e^{k(\hat{a}^\dagger \hat{a} - \hat{b}^\dagger \hat{b})(\hat{c} \eta(t) - \hat{c}^\dagger \eta(t)^*)} = \\ &= e^{-it} e^{-k(\hat{a}^\dagger \hat{a} - \hat{b}^\dagger \hat{b})(\hat{c} \eta(t) - \hat{c}^\dagger \eta(t)^*)} \hat{c} e^{k(\hat{a}^\dagger \hat{a} - \hat{b}^\dagger \hat{b})(\hat{c} \eta(t) - \hat{c}^\dagger \eta(t)^*)} = \hat{c} e^{-it} - k\eta(t)^* e^{-it} (\hat{a}^\dagger \hat{a} - \hat{b}^\dagger \hat{b}), \end{aligned} \quad (\text{S29})$$

which leads to the desired result after noting that $-\eta(t)^* e^{-it} = \eta(t)$.

IV. QUANTIFYING ENTANGLEMENT AND ENTROPY FOR GAUSSIAN STATES

To quantify entanglement for all bipartite subsystems we employed the logarithmic negativity, as it is an entanglement monotone [44] and efficiently computable for Gaussian states. The initial state of the system is assumed to be:

$$\rho_0 = |\alpha\rangle \langle \alpha| \otimes |\beta\rangle \langle \beta| \otimes \rho_{th}, \quad (\text{S30})$$

where the cavity modes are in a coherent state and the mirror is in a thermal state $\rho_{th} \propto \exp\left(-\frac{\hbar\omega_m \hat{c}^\dagger \hat{c}}{k_B T}\right)$. All modes and bipartite subsystems are initially in Gaussian states; moreover, the unitary evolution operator (S22) preserves Gaussianity, so both quantities above can be computed from the covariance matrix of the subsystem [44, 45].

Considering \hat{a}_1 and \hat{a}_2 to be the annihilation operators of any of the bipartite subsystems, we define their corresponding quadrature field operators as $\hat{Q}_i = \hat{a}_i + \hat{a}_i^\dagger$, $\hat{P}_i = i(\hat{a}_i^\dagger - \hat{a}_i)$ and the formal vector $\hat{x} = (\hat{Q}_1, \hat{P}_1, \hat{Q}_2, \hat{P}_2)$ such that the covariance matrix for this subsystem is defined as:

$$V_{i,j} = \frac{1}{2} \langle \hat{x}_i \hat{x}_j + \hat{x}_j \hat{x}_i \rangle - \langle \hat{x}_i \rangle \langle \hat{x}_j \rangle. \quad (\text{S31})$$

We note that the time-dependent expectation values can be calculated from the initial state ρ_0 using the Heisenberg picture, see equations (S24) - (S26). It is useful to rewrite the covariance matrix in terms of its 2×2 submatrices V_1, V_2, V_3 :

$$V = \begin{bmatrix} V_1 & V_3 \\ V_3^T & V_2 \end{bmatrix}. \quad (\text{S32})$$

To compute the von Neumann entropy, we first define $\Delta \equiv \det(V_1) + \det(V_2) + 2\det(V_3)$ and calculate the symplectic eigenvalues of V , given by [45]

$$\nu_{\pm} = \sqrt{\frac{\Delta \pm \sqrt{\Delta^2 - 4\det(V)}}{2}}. \quad (\text{S33})$$

Defining $g(x) \equiv \left(\frac{x+1}{2}\right) \log\left(\frac{x+1}{2}\right) - \left(\frac{x-1}{2}\right) \log\left(\frac{x-1}{2}\right)$, the von Neumann entropy S is then given by [44]

$$S = \sum_{k=1}^N g(\nu_k). \quad (\text{S34})$$

The logarithmic negativity can be computed as

$$E_N = \max(0, -\log(\tilde{\nu}_-)), \quad (\text{S35})$$

where $\tilde{\nu}_-$ is the smallest of the symplectic eigenvalues of the covariance matrix calculated with respect to the partial transpose of the reduced density matrix of the subsystem under discussion [45]. In practice, the effect of the partial transposition mentioned above is that the symplectic eigenvalues of \tilde{V} differ from equations (S33) by a sign change in $\det(V_3)$,

$$\tilde{\nu}_{\pm} = \sqrt{\frac{\sigma \pm \sqrt{\sigma^2 - 4\det(V)}}{2}}, \quad (\text{S36})$$

where $\sigma = \det(V_1) + \det(V_2) - 2\det(V_3)$.

To compute the covariance matrices, we proceeded by calculating the averages of all quadratic expressions in $\hat{a}, \hat{b}, \hat{c}$ and their adjoints. By applications of identities already mentioned in the previous section, together with the displacement relation $\hat{c}\hat{\mathcal{D}}_C(\kappa)(\kappa) = \hat{\mathcal{D}}_C(\kappa)(\kappa)(\hat{c} + \kappa)$, we find the following expressions for $\hat{a}(t)^2$, $\hat{b}(t)^2$, $\hat{c}(t)^2$, $\hat{a}(t)\hat{b}(t)$, $\hat{a}(t)\hat{b}^\dagger(t)$, $\hat{a}(t)\hat{c}(t)$, $\hat{a}(t)\hat{c}^\dagger(t)$, $\hat{b}(t)\hat{c}(t)$, $\hat{b}(t)\hat{c}^\dagger(t)$ and $\hat{c}^\dagger(t)\hat{c}(t)$,

$$\hat{a}(t)^2 = e^{-2ir_a t} e^{-4iB(t)} e^{4iB(t)\hat{b}^\dagger\hat{b}} e^{-4iB(t)\hat{a}^\dagger\hat{a}} \hat{\mathcal{D}}_C(\kappa)(+2k\xi(t))\hat{a}^2 \quad (\text{S37})$$

$$\hat{b}(t)^2 = e^{-2ir_b t} e^{-4iB(t)} e^{4iB(t)\hat{a}^\dagger\hat{a}} e^{-4iB(t)\hat{b}^\dagger\hat{b}} \hat{\mathcal{D}}_C(\kappa)(-2k\xi(t))\hat{b}^2 \quad (\text{S38})$$

$$\hat{c}(t)^2 = \hat{c}^2 e^{-2it} + 2ke^{-it}(\hat{a}^\dagger\hat{a} - \hat{b}^\dagger\hat{b})\eta(t)\hat{c} + k^2(\hat{a}^\dagger\hat{a} - \hat{b}^\dagger\hat{b})^2\eta(t)^2 \quad (\text{S39})$$

$$\hat{a}(t)\hat{b}(t) = e^{-(r_a+r_b)t}\hat{a}\hat{b} \quad (\text{S40})$$

$$\hat{a}(t)\hat{b}^\dagger(t) = e^{i(r_b-r_a)t}\hat{b}^\dagger e^{4iB(t)\hat{b}^\dagger\hat{b}} e^{-4iB(t)\hat{a}^\dagger\hat{a}} \hat{\mathcal{D}}_C(\kappa)(2k\xi(t))\hat{a} \quad (\text{S41})$$

$$\begin{aligned} \hat{a}(t)\hat{c}(t) &= e^{-i(r_a t+B(t))} e^{-it} e^{2iB(t)\hat{b}^\dagger\hat{b}} e^{-2iB(t)\hat{a}^\dagger\hat{a}} \hat{\mathcal{D}}_C(\kappa)(+k\xi(t))\hat{a}\hat{c} + \\ &e^{-i(r_a t+B(t))} e^{2iB(t)\hat{b}^\dagger\hat{b}} e^{-2iB(t)\hat{a}^\dagger\hat{a}} \hat{\mathcal{D}}_C(\kappa)(+k\xi(t))k(\hat{a}^\dagger\hat{a} - \hat{b}^\dagger\hat{b} + I)\hat{a}\eta(t) \end{aligned} \quad (\text{S42})$$

$$\begin{aligned} \hat{a}(t)\hat{c}^\dagger(t) &= e^{-i(r_a t+B(t))} e^{it} e^{2iB(t)\hat{b}^\dagger\hat{b}} e^{-2iB(t)\hat{a}^\dagger\hat{a}} \hat{\mathcal{D}}_C(\kappa)(+k\xi(t))\hat{a} + \\ &e^{-i(r_a t+B(t))} e^{2iB(t)\hat{b}^\dagger\hat{b}} e^{-2iB(t)\hat{a}^\dagger\hat{a}} \hat{\mathcal{D}}_C(\kappa)(+k\xi(t))k(\hat{a}^\dagger\hat{a} - \hat{b}^\dagger\hat{b})\hat{a}\eta(t)^* \end{aligned} \quad (\text{S43})$$

$$\begin{aligned} \hat{b}(t)\hat{c}(t) &= e^{-i(r_b t+B(t))} e^{-it} e^{2iB(t)\hat{a}^\dagger\hat{a}} e^{-2iB(t)\hat{b}^\dagger\hat{b}} \hat{\mathcal{D}}_C(\kappa)(-k\xi(t))\hat{b}\hat{c} + \\ &e^{-i(r_b t+B(t))} e^{2iB(t)\hat{a}^\dagger\hat{a}} e^{-2iB(t)\hat{b}^\dagger\hat{b}} \hat{\mathcal{D}}_C(\kappa)(-k\xi(t))k(\hat{a}^\dagger\hat{a} - \hat{b}^\dagger\hat{b} - I)\hat{b}\eta(t) \end{aligned} \quad (\text{S44})$$

$$\begin{aligned} \hat{b}(t)\hat{c}^\dagger(t) &= e^{-i(r_b t+B(t))} e^{it} e^{2iB(t)\hat{a}^\dagger\hat{a}} e^{-2iB(t)\hat{b}^\dagger\hat{b}} \hat{\mathcal{D}}_C(\kappa)(-k\xi(t))\hat{b} + \\ &e^{-i(r_b t+B(t))} e^{2iB(t)\hat{a}^\dagger\hat{a}} e^{-2iB(t)\hat{b}^\dagger\hat{b}} \hat{\mathcal{D}}_C(\kappa)(-k\xi(t))k(\hat{a}^\dagger\hat{a} - \hat{b}^\dagger\hat{b})\hat{b}\eta(t)^* \end{aligned} \quad (\text{S45})$$

$$\hat{c}^\dagger(t)\hat{c}(t) = \hat{c}^\dagger\hat{c} + k(\hat{a}^\dagger\hat{a} - \hat{b}^\dagger\hat{b})(\hat{c}^\dagger\xi(t) + \hat{c}\xi(t)^*) + k^2(\hat{a}^\dagger\hat{a} - \hat{b}^\dagger\hat{b})^2|\xi(t)|^2 \quad (\text{S46})$$

The operators $\hat{a}^\dagger\hat{a}$ and $\hat{b}^\dagger\hat{b}$ commute with H , so are constant. All the remaining quadratic expressions follow from the equations above by commutation or by considering the adjoint equations - we then compute the average values of those expressions with respect to the state ρ_0 of the system, and finally the covariance matrices for the three bipartite subsystems.

It is useful to write the thermal state ρ_{th} in the coherent state basis of the mechanical oscillator,

$$\rho_{th} = \int \frac{d^2\gamma}{\pi\bar{n}} e^{-\frac{|\gamma|^2}{\bar{n}}} |\gamma\rangle \langle\gamma|, \quad \text{where } \bar{n} = \text{Tr}(\rho_{th}\hat{c}^\dagger\hat{c}). \quad (\text{S47})$$

Then, for every operator \hat{A} , the average value with respect to ρ_0 is

$$\langle\hat{A}\rangle = \text{Tr}(\rho_0\hat{A}) = \int \frac{d^2\gamma}{\pi\bar{n}} e^{-\frac{|\gamma|^2}{\bar{n}}} \langle\alpha, \beta, \gamma| \hat{A} |\alpha, \beta, \gamma\rangle. \quad (\text{S48})$$

In what follows, we take advantage of the eigenvalue equations

$$\hat{a}|\alpha, \beta, \gamma\rangle = \alpha|\alpha, \beta, \gamma\rangle, \quad \hat{b}|\alpha, \beta, \gamma\rangle = \beta|\alpha, \beta, \gamma\rangle, \quad \hat{c}|\alpha, \beta, \gamma\rangle = \gamma|\alpha, \beta, \gamma\rangle. \quad (\text{S49})$$

and the dual equations

$$\langle \alpha, \beta, \gamma | \hat{a}^\dagger = \alpha^* \langle \alpha, \beta, \gamma | \quad , \quad \langle \alpha, \beta, \gamma | \hat{b}^\dagger = \beta^* \langle \alpha, \beta, \gamma | \quad , \quad \langle \alpha, \beta, \gamma | \hat{c}^\dagger = \gamma^* \langle \alpha, \beta, \gamma | \quad . \quad (\text{S50})$$

By Gaussian integrals

$$\langle \hat{c}^m \rangle = \int \frac{d^2 \gamma}{\pi \bar{n}} \exp\left(-\frac{|\gamma|^2}{\bar{n}}\right) \gamma^m = \delta_{m,0} \quad , \quad (\text{S51})$$

$$\langle \hat{\mathcal{D}}_C(\kappa) \rangle = \int \frac{d^2 \gamma}{\pi \bar{n}} \exp\left(-\frac{|\gamma|^2}{\bar{n}}\right) \langle \gamma | \hat{\mathcal{D}}_C(\kappa) | \gamma \rangle = e^{-\frac{|\kappa|^2}{2}} e^{-\bar{n}|\kappa|^2} \quad , \quad (\text{S52})$$

$$\langle \hat{\mathcal{D}}_C(\kappa) \hat{c} \rangle = \int \frac{d^2 \gamma}{\pi \bar{n}} \exp\left(-\frac{|\gamma|^2}{\bar{n}}\right) \gamma \langle \gamma | \hat{\mathcal{D}}_C(\kappa) | \gamma \rangle = \bar{n} \kappa e^{-\frac{|\kappa|^2}{2}} e^{-\bar{n}|\kappa|^2} \quad . \quad (\text{S53})$$

The following relations are also useful,

$$\langle \exp(if(t) \hat{a}^\dagger \hat{a}) \rangle = \exp\left(-|\alpha|^2 (1 - e^{if(t)})\right) \quad (\text{S54})$$

$$\langle \exp(if(t) \hat{a}^\dagger \hat{a}) \hat{a}^\dagger \hat{a} \rangle = |\alpha|^2 e^{if(t)} \exp\left(-|\alpha|^2 (1 - e^{if(t)})\right) \quad (\text{S55})$$

as well as the analogous expressions for \hat{b} , with β replacing α . The first one follows from Taylor expanding the exponential, while the second follows from the first by commuting \hat{a}^\dagger to the left with the adjoint of equation (S27). The identity below is trivial to check:

$$\langle (\hat{a}^\dagger \hat{a} - \hat{b}^\dagger \hat{b})^2 \rangle = (|\alpha|^2 - |\beta|^2)^2 - (|\alpha|^2 + |\beta|^2) \quad (\text{S56})$$

Applying the identities above to the expressions for the quadratic terms in the annihilation and creation operators, we compute the matrix elements of all three covariance matrices and therefore quantify entanglement for all bipartite subsystems by calculating the von Neumann entropies and the logarithmic negativities.

V. COUPLING DEPENDENCE

The fundamental building blocks needed to calculate the logarithmic negativity and von Neumann entropy are the entries of the covariance matrix. The general behavior of these expectation values can be exemplified through the following correlator, shown in the “real” non-scaled time below:

$$\begin{aligned} \langle \hat{a}(t) \hat{b}(t)^\dagger \rangle &= \alpha \beta^* e^{-i(r_a - r_b)\omega_m t} e^{-|\beta|^2 [1 - e^{4iB(\omega_m t)}]} \\ &\quad e^{-|\alpha|^2 [1 - e^{-4iB(\omega_m t)}]} e^{-k^2 |\eta(\omega_m t)|^2 [4\bar{n} + 2]} \quad . \end{aligned} \quad (\text{S57})$$

The entanglement and entropy of the subsystems is, thus, given by a product of terms of the form:

1. $e^{ir_a \omega_m t}, e^{ir_b \omega_m t}, e^{i(r_a \pm r_b)\omega_m t}, \dots$: result of the free evolution;
2. $e^{-|\alpha|^2 [1 - e^{-2niB(\omega_m t)}]} e^{-|\beta|^2 [1 - e^{2niB(\omega_m t)}]}$, $n = 1, 2$: result of the interaction on coherent states;
3. $e^{-k^2 |\eta(\omega_m t)|^2 [4n\bar{n} + \frac{1}{2}]}$, $n = 1, 4$: result of the interaction on thermal state.

Considered the order of magnitude of the experimental parameters used in the main text, $\omega_a = \omega_b \sim 10^{15}$, $\omega_m \sim 10^5$ Hz, the free evolution terms oscillate very rapidly compared to the others and can be approximated on average as constant. Consequently, the general periodicity of the entanglement and entropy are dictated solely by the periodicity of the thermal and coherent terms, given by $\tau_1 = 2\pi/\omega_m$ and $\tau_2 = \pi/\omega_m k^2$, respectively.

When $\tau_1 \ll \tau_2 \Rightarrow k \ll 1/\sqrt{2}$, the “low coupling” regime, the coherent terms dominate the overall form of the logarithmic negativity and entropy, while the thermal terms describe fine oscillations. Therefore the periodicity of

entanglement and entropy is $\tau = \pi/\omega_m k^2$. Numerically, we have observed that the maximum of the logarithmic negativity within one period τ is mostly constant, but since the period of entanglement grows with $1/k^2$ as k goes to 0, it becomes potentially much larger than the lifetime of a photon inside the optical cavities and becomes impossible to observe.

When $\tau_1 \gg \tau_2 \Rightarrow k \gg 1/\sqrt{2}$, the “high coupling” regime, the thermal terms dominate the overall form of the logarithmic negativity and entropy, while the coherent terms describe fine oscillations. Therefore the periodicity of entanglement and entropy is $\tau = 2\pi/\omega_m$. Numerically, we have observed that the maximum of the logarithmic negativity within one period τ is very sensitive to small changes of k , presenting local minima many orders of magnitude smaller than at its surrounding when $\tau_1 = N\tau_2 \Rightarrow 2k^2 = N$, $N \in \mathbb{N}^*$. As k grows much bigger than 1, any small change in k can easily throw the logarithmic negativity into a much smaller value than its surroundings.